

New Methodology Surface to Hole for the Detection of Deep Conductors around Drillholes Using D.C Methods: Case Study from Rouez Mine, Bretagne, France

JAMAL ASFAHANI

*Geology Department, Atomic Energy Commission
Damascus, Syria*

Received: 1/1/2002

Revised: 22/5/2002

Accepted: 23/10/2002

ABSTRACT. A new geoelectrical configuration, surface to hole for the detection of deep conductors around drillholes, using the D.C. has been proposed. This new configuration is characterized by its high depth penetration compared with the other known traditional geoelectrical methods, applied from surface and in the wells. It presents a directional effect, which is one of the most important advantages of this configuration that proves its superiority. This configuration has been tested in the Rouez mine, Bretagne, France, where sulphide mineralisation is known to occur. Several anomalies have been isolated in the field data and interpreted by different interpretative techniques. The results obtained by applying this configuration were concordant and the detected conductors were approved by morphological and lithological descriptions.

Introduction

Since not long time ago, the used techniques for mineral prospecting allowed only to discover surfacial mines. Recently, the development of structural and applied geophysics has made the exploiting of very deep mines possible. Today, it is necessary to develop several methods to investigate very deep mines, but unfortunately the physical nature of the phenomenon, which allows the detection from surface, has raised a real problem related to the penetration depth. In fact, it is impossible in most cases to determine a mineral body, having more depth than its dimension. Thus, it is urgent to use drill holes to know and to

evaluate such mineral body. Wells drilling stage comes after the application of surface geoelectrical measurements. Usually, geophysicists interpret the results by trying to get the highest quantity information as possible as they could. This will lead finally to determine the location of the well that should be drilled. Unfortunately, the first well can not reach the objective body due to the existence of many bodies or overburden having a high conductivity. Furthermore, the high depth of the body complicates the problem from an interpretation point of view. In attempt to obtain accurate results regarding the identification of a mineral body, geophysicists have been trying for a long time to use the wells for geophysical measurements. In fact, using of wells allows obtaining more depth penetration than that obtained by surface geoelectrical methods. However, the reached depth penetration around the well is expected to be not more than 30 cm. But, it is useful to know the nature of the penetrated formation by the well with a good accuracy. The adjacent and far formations from the well can not be detected by the conventional resistivity well logging. Recent geophysical researches are directed towards the development of new methods to investigate mainly deep conductive bodies existing nearby but not intersected by the studied well. From an economic point of view, it is also useful to develop methods to reduce the number of necessary wells.

Geoelectrical surface to hole measurements hold today the attention of many geophysicists. Several electrodes configurations have been tested, (Yang and Ward, 1985; Dobecki, 1980; Daniels, 1978; and Daniels, 1983). The use of apparent resistivity notion is well adapted to one-dimensional interpretation of surface geoelectrical investigation. From the use of this apparent resistivity notion some problems arise in the surface to hole applications where 3D consideration should be taken into account.

The main purpose of this paper is to introduce a new hole to surface geoelectrical configuration using DC. This configuration is theoretically investigated (Asfahani, 1989, and Florsh, 1986) in order to specify the characteristics of obtained anomaly in the case of a conductive sphere, not intersecting with the well, and undergoing to uniform electrical field. The validity of such a configuration is successfully tested in the Rouez mine in France Asfahani, 1989, where sulphide mineralization is known to occur.

Characteristics of the New Hole to Surface Configuration

The new configuration introduced in this research aims mainly to detect the deep conductors not intersected with the wells. It consists of:

- 1) Injecting the electrical current at the ground surface between two electrodes A and B, which are symmetrically situated with respect to the top of the well: (i.e. $AO = OB$)

2) Measuring the potential difference between two electrodes M and N, which are incorporated into a movable downhole tool in the well, as shown in Fig. 1. The geometric coefficient of such a configuration tends to be infinite, therefore the apparent resistivity notion could not be used when applying this configuration, and the vertical electrical gradient is obtained and used instead of traditional apparent resistivity.

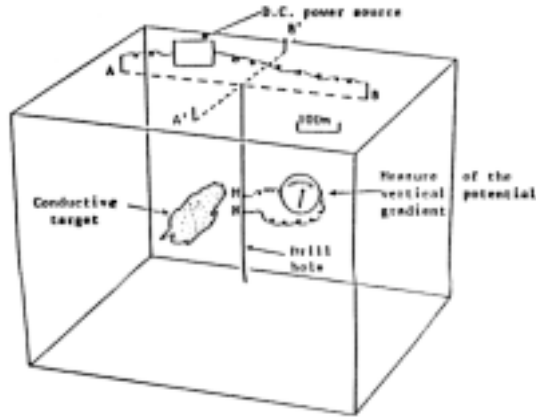


FIG. 1. The new proposed surface to well configuration.

The new configuration proposed in this study could be qualified as a null response system in a homogeneous or uniformly layered earth. This configuration will therefore respond when the current distribution is disturbed by a source of secondary or perturbation potential. Otherwise, the measuring of vertical electrical component in the well indicates the presence of inhomogeneous underground. The role of the proposed configuration is to determine its characteristics, including essentially the depth, the distance between the center of this inhomogeneity and the studied well, and finally the directional azimuth, which could be obtained by using this configuration.

In this new applied method in the wells, two vertical electrical gradient curves are obtained; the first one is obtained when the current is injected at the ground surface in the EW direction. The second one is obtained when the current is injected at the ground surface in the NS direction, Asfahani, 1989. Obtaining two vertical electrical gradients A_{EW} and A_{NS} curves in the well allows to determine the azimuth of the conductive body. The azimuth determination gives this configuration its superiority in comparison with other geoelectrical configurations applied in the surface and in the wells.

A theoretical study was conducted to know the characteristics of the vertical electrical gradient curves obtained in the case of presence of a conductive sphere not intersected with the well, and undergoing to the uniform and hor-

horizontal field (Asfahani, 1989; and Florsh, 1986). The shape of the vertical electrical gradient curve resulting from the application of this configuration is extremely simple and is characterized as follows:

– It has one maximum and one minimum, the vertical distance "d" between them is the same as the theoretical distance between the well and the sphere center, Fig. 2.

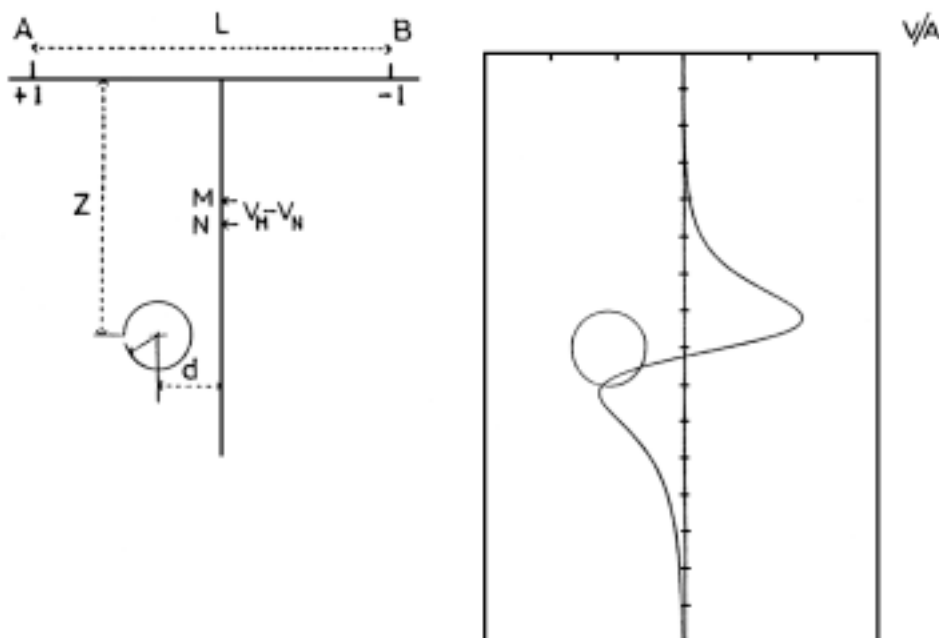


FIG. 2. The response characteristic of the proposed configuration.

– The vertical electrical gradient is equal to zero at the depth corresponding to the theoretical depth of the sphere center (Z).

– The azimuth of the conductive sphere could be easily obtained, as we will show later.

The primary horizontal electrical field needed for such a configuration is attenuated as a function of depth. This attenuation can be demonstrated by writing the potential expression at the vicinity of the well in the following form:

$$V(x, Z_i) = \frac{I\rho}{2\pi} \left[\frac{1}{\sqrt{\left(\frac{L}{2} - X\right)^2 + Z_i^2}} - \frac{1}{\sqrt{\left(\frac{L}{2} + X\right)^2 + Z_i^2}} \right] \quad [1]$$

- Where ρ : is the resistivity surrounding Fig. 3a.
 L : The distance between the two current electrodes A and B.
 Z_i : Variable depth.
 X : Variable in the X direction.
 I : Intensity of electrical current.

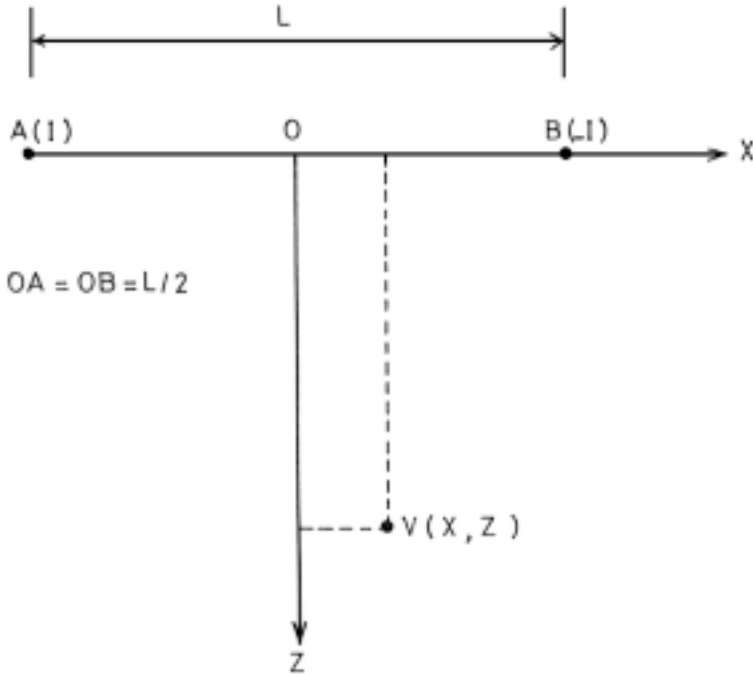


FIG. 3a. The geometry for the computation of the potential at the point (x,z) .

The horizontal field in the well as a function of the depth (Z_i) is given by the derivation of the equation [1] as a function of (x) :

$$E(Z_i) = \left[\frac{\partial V}{\partial X} \right]_{X=0} = \frac{\left(\frac{L}{2}\right)I\rho}{\pi \left[\left(\frac{L}{2}\right)^2 + Z_i^2 \right]^{3/2}} \quad [2]$$

The variation of the equation [2] shown in Fig. 3b indicates clearly the decrease of the primary field as a function of depth. The secondary electrical field resulting from the presence of a conductive structure is influenced by this decrease. Therefore, the amplitude of the measured anomaly is as weak as the structure is deep. This attenuation must be taken in consideration, and the field data have to be therefore corrected by introducing a corrective factor (CF), which has the following formula:

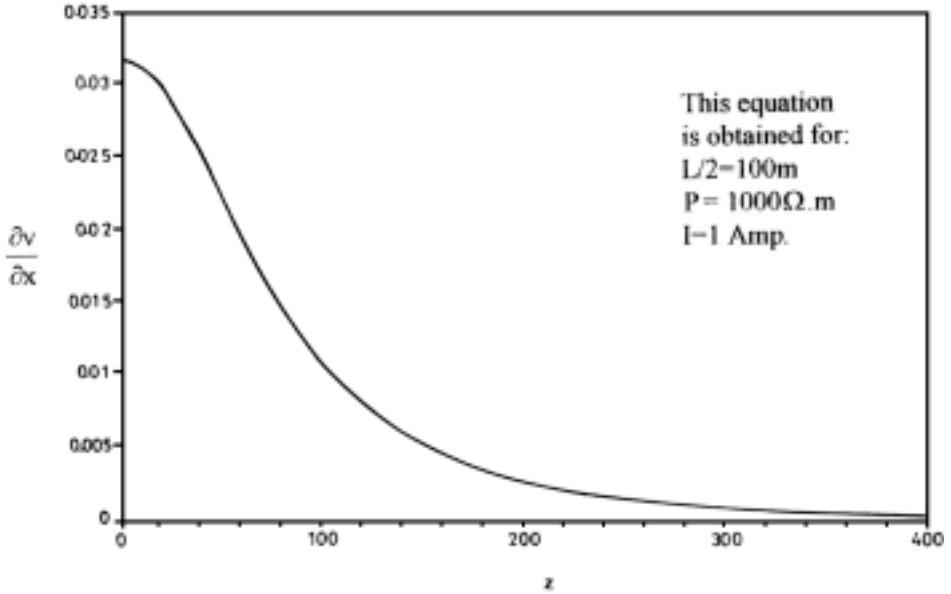


FIG. 3b. The variation of the horizontal field as a function of depth.

$$CF = \frac{\left[\left(\frac{L}{2} \right)^2 + Z_i^2 \right]^{1.5}}{\left[\frac{L}{2} \right]^3} \quad [3]$$

The “CF” is chosen to be equal to 1 at the ground surface ($Z_i = 0$).

Optimal Distance "L" between Current Electrodes A and B

It is extremely necessary to select an optimum distance "L" between the two electrodes A and B at the surface for detecting a conductor located at depth Z_i . This optimum distance can be obtained by deriving equation [2] as a function of "L" and putting zero value to this derivative as follows:

$$\frac{\partial E(Z_i)}{\partial L} = \left[\frac{\left(\left(\frac{L}{2} \right)^2 + Z_i^2 \right) - 3 * \left(\frac{L}{2} \right)^2}{\left[\left(\frac{L}{2} \right)^2 + Z_i^2 \right]^{2.5}} \right] \quad [4]$$

$$\frac{\partial E}{\partial L} = 0 \Rightarrow L = \sqrt{2} * Z_i \quad [5]$$

Equation [5] indicates clearly the relationship between L and Z , so L can be adapted as a function of the expected target depth Z_i .

Azimuth Determination

The new proposed configuration in this research has the advantage and the superiority in comparison with other geoelectrical methods in the determination of the azimuth of the conductive body. In order to determine the azimuth direction of the conductive body, the following notions have to be assumed in practical field:

- 1) The positive current (+) is placed in the West, when the electrical current is injected in the EW direction, and placed in the North, when the electrical current is injected in the NS direction, Fig 4a.
- 2) The negative current (–) is placed in the East, when the electrical current is injected in the EW direction, and placed in the South, when the electrical current is injected in the NS direction, Fig 4a.
- 3) The positive electrode of the potential in the well is situated over the negative one.

Fig. 4a shows the possibilities of the position of a conductive sphere in the plane. The plane around the well could be divided into four zones. Each of them is characterized by specific vertical gradient curves, Fig 4b, according to the polarity of the electrical current.

Let (φ) is supposed to be the angle between the plane containing the conductive sphere from one side and the plane containing both the studied well and the line corresponding to the EW current injection direction from the other side. The main goal is therefore to determine (φ) from vertical gradient curves obtained according to EW and NS directions.

The amplitudes of the anomalies obtained according to the current injection in EW and NS directions are respectively:

$$\bar{A}_{EW} = \bar{A} \cos(\varphi) \quad [6]$$

$$\bar{A}_{NS} = \bar{A} \sin(\varphi) \quad [7]$$

Where \bar{A} is the resulting anomaly given by the following relationship, Fig. 5.

$$\bar{A} = \sqrt{\bar{A}_{EW}^2 + \bar{A}_{NS}^2} \quad [8]$$

From the equations [6] and [7], it is easy to write the following:

$$\frac{\bar{A}_{NS}}{\bar{A}_{EW}} = \operatorname{tg}\varphi \quad [9]$$

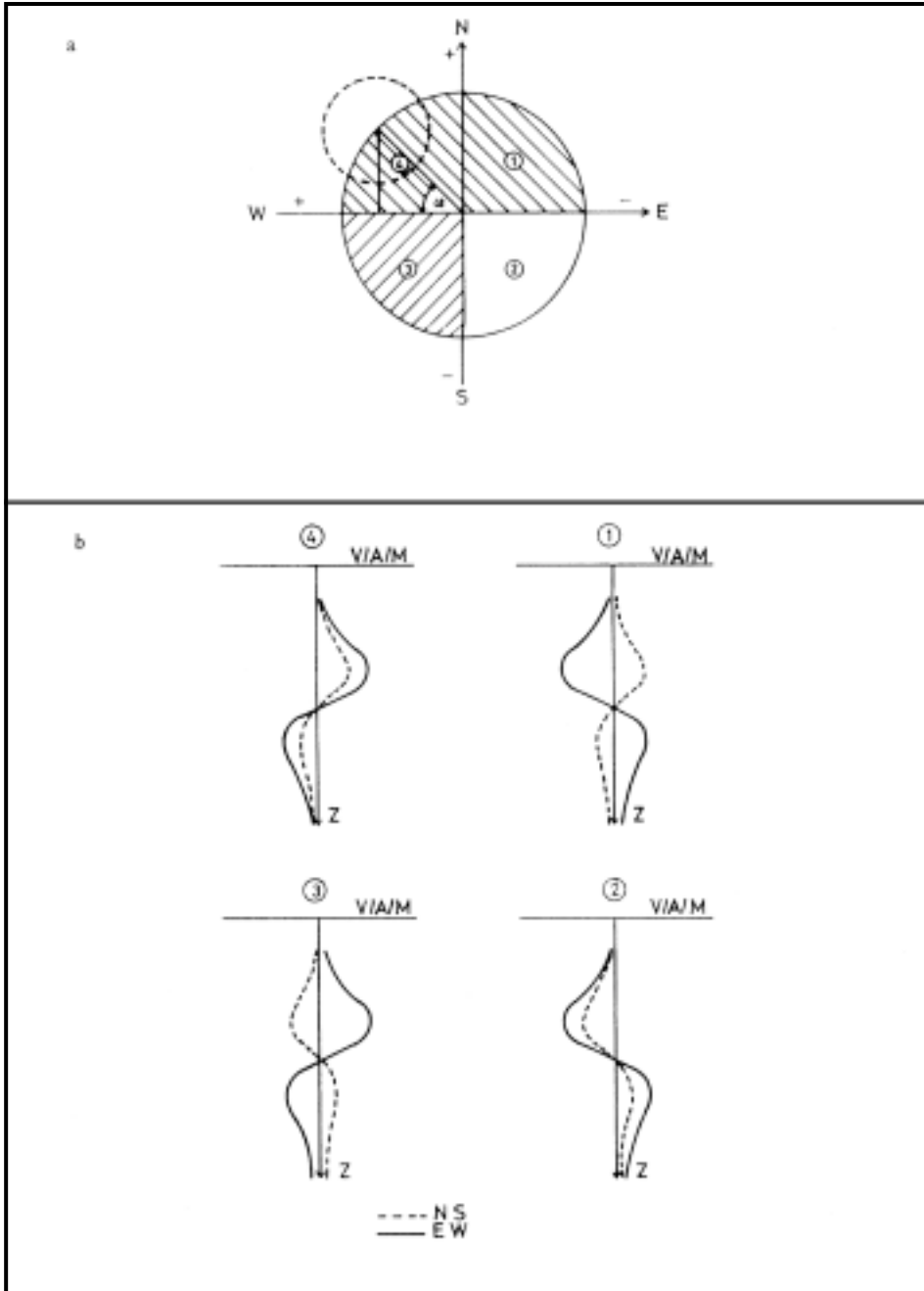


FIG. 4a. The position of the conductive sphere around the well according to the current injection.
 b. Characteristics of vertical gradient curves, representing each of the four zones.

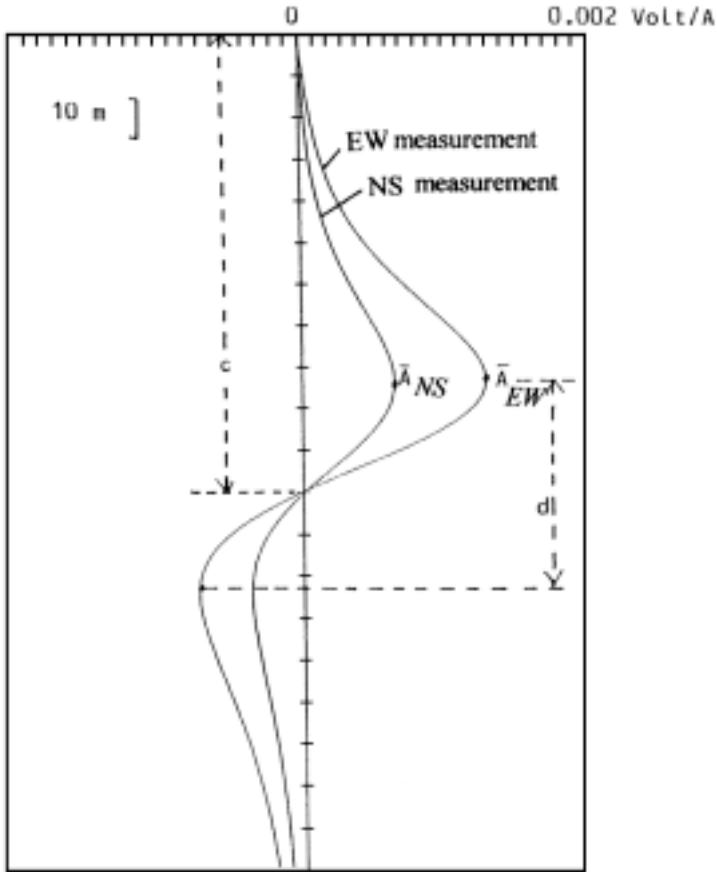


Fig. 5. Synthetic example shows the azimuth determination.

Equation [9] allows the determination of (φ) as follows:

$$\varphi = \text{arctg} \frac{A_{NS}}{A_{EW}} \quad [10]$$

Fig. 5 shows a synthetic example concerning the azimuth determination. This synthetic example is obtained by using the following assumed parameters:

- Distance between the two electrodes of injection current $L = 200\text{ m}$
- Intensity of electrical current $I = 1\text{ Amp}$
- Resistivity of the host rocks $\rho_1 = 1000\ \Omega \cdot \text{m}$
- Azimutal angle $\varphi = 30^\circ$
- Radius of the conductive sphere $r = 25\text{ m}$ and
- Depth of the sphere center $Z = 100\text{ m}$.

From these assumed parameters, we obtain the following:

$$A_{NS} = 6.5 * 10^{-4}, A_{EW} = 12.75 * 10^{-4} \Rightarrow \bar{A} \sqrt{A_{NS} + A_{EW}} = 1.43 * 10^{-3}$$

Using equation [10], the azimuthal angle can be obtained as follows:

$$\varphi = \text{tg}^{-1} \frac{6.5}{12.75} = 27^\circ$$

Interpretative Techniques

Through the theoretical study of this configuration, the obtained theoretical anomaly is identified by extreme simplicity in the case of a conductive sphere not intersected with the well, Asfahani, 1989 and Florsh, 1986. The real problem is raised when this new configuration is applied in the field, due to the complexity of the geological and structural conditions of the mining sites. The vertical electrical gradient curves obtained in the field are therefore extremely complex, and their interpretation is not an easy task.

Being a new proposed configuration, therefore, the vertical electrical gradient curves have to be prepared for interpretation in two phases:

The first phase includes both the data correction for electrical field attenuation and the filtering of these corrected data. The second phase includes mainly the interpretation of corrected and filtered field data by different developed methodologies (Chart and inversion methods).

Filtering Technique

The vertical electrical gradient curve obtained by the new proposed configuration contains overlapping of anomalies having different wavelengths. The recursive filters are used in order to separate these anomalies to different ones. In fact, this filtering procedure is easily applicable, permits to select the distance to the well that we want to look for. Since the wavelength of the anomaly increases with the well to conductor distance. Therefore, the main objective is to separate these overlapped anomalies to different ones, not as a function of wavelength (λ) but as a function of a distance between the studied well and the conductor (d). By this manner, a kind of cartography of existed conductors could be obtained as a function of distance.

The potential anomaly due to the presence of a conductive sphere not intersected with the well is given by the following relationship (Asfahani,1989):

$$V(Z_i) = \frac{1}{(d^2 + Z_i^2)^{1.5}} \quad [11]$$

Where d : is the distance between well and sphere center.

Z_i : Variable depth

It is therefore interesting to know the spectral continuation of the obtained anomaly $V(Z_i)$, due to the conductive sphere not intersected with the well.

The Fourier transform $F(W)$ of the obtained anomaly $V(Z)$, in a continuous form is given by the following equation Asfahani, 1989 and Florsh, 1986:

$$F(W) = \int_{-\infty}^{+\infty} \frac{e^{-iWz}}{(d^2 + Z^2)^{1.5}} dz = 2 \int_0^{\infty} \frac{\cos(Wz)}{(d^2 + z^2)^{1.5}} dz \quad [12]$$

Where : $w = \frac{2\pi}{\lambda}$

After developing [12] by using Tables of integrals (Gradshteyn *et al.*, 1969), it was found that the maximum spectral of $F(W)$ is situated at $w = 1.332$, for $d = 1$, which allows to obtain the following relationship:

$$\lambda = 4.717 d \quad [13]$$

Three types of filters have been applied to the corrected field data. These filters are:

- The first filter is characterized as follows: $4 < d < 16$ m, and aimed at selecting the short- wavelengths anomalies.
- The second filter is characterized as follows: $16 < d < 64$ m, and aimed at selecting the intermediate wavelengths anomalies.
- The third low pass filter is characterized as follows: $d > 64$ m, and aimed at selecting the long- wavelengths anomalies.

These three filters have been applied on the real field data obtained by using the new hole to surface configuration in the Rouez mine.

Chart Method

Chart method is developed by Florsh 1986, for the interpretation of the results obtained by this configuration. Using a set of charts, the perfectly conductive spherical model in a uniform half space was employed.

Two suppositions are taken in consideration:

The resistivity of the host rocks (ρ_1) is known. In fact, it can be obtained by traditional geoelectrical well logging.

The resistivity contrast (ρ_1/ρ_2) is bigger than 10, (ρ_2) is the resistivity of the conductive target.

The chart method permits the determination of the depth (Z), azimuthal angle (φ), distance to the well (d), and radius of the sphere (r).

Fig. 6 illustrates the application of this method on a synthetic example. This method uses two kinds of charts, A and B. Chart A is established in order to obtain the radius of the conductive sphere (r) as follows:

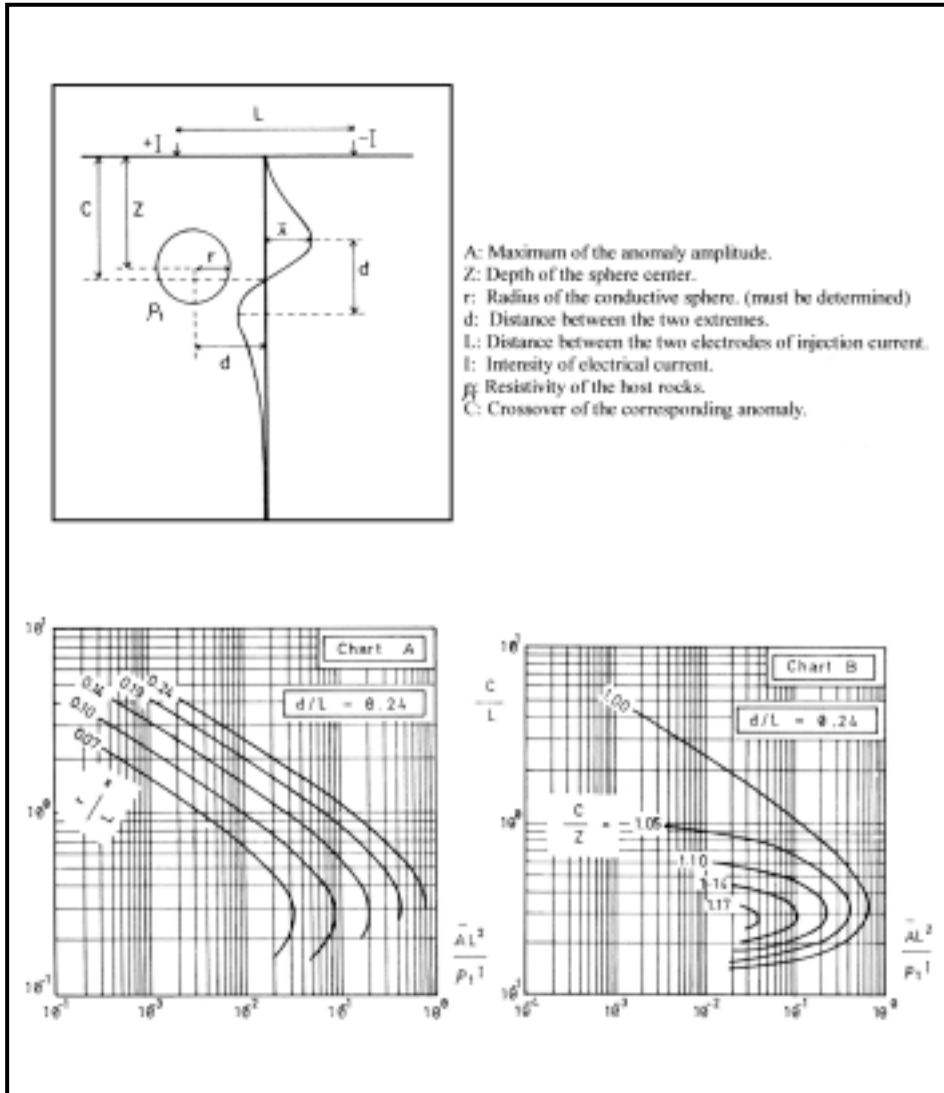


FIG. 6. Chart method and an example of interpretation.

We select the Chart A coresponding to $d/L=50/200 = 0.25$ (d is the distance between the two extremes as shown in Fig. 5). We need also to compute both the ratio $\frac{A_{\mathcal{L}}}{\rho_1 I}$ and the ratio C/L (C is the cross-over depth of the coresponding anomaly). $\frac{A_{\mathcal{L}}}{\rho_1 I} = 0.057$ and $C/L = 110/200 = 0.55$ (C is equal to 110 m as shown in Fig. 5).

The intersection point of (0.057 and 0.55) allows to obtain the ratio r/L of 0.12 Fig. 6.

$$\frac{r}{L} = 0.12 \Rightarrow r = 24 \text{ m}$$

Chart B is formulated in order to obtain the depth of the sphere center (Z), and used by the same manner as Chart A. The intersection point of (0.057 and 0.55) allows to obtain the ratio C/Z of 1.09

$$\frac{C}{Z} = 1.09 \Rightarrow Z = 101 \text{ m}$$

Inverse Method

This method is commonly used in applied geophysics, and consists of finding a theoretical model, which matches the corrected field data. The spherical model in the presence of a uniform primary electrical field is used in inversion procedure. The mathematical inverse problem has been developed in this research in order to evaluate the parameters of the spherical model ($Z, d, r, \rho_1, \rho_2, \varphi$)

These parameters could be obtained by minimizing the following function:

$$\text{Min } f(Z, d, r, \rho_1, \rho_2, \varphi^0) = \text{Min } \sum_{i=1}^{i=n} \left[L(X_i) - V(X_i, Z, d, r, \rho_1, \rho_2, \varphi^0) \right]^2$$

Where: $L(X_i) = 1, \dots, n$ are the measured values of potential anomaly at the points $X_i = 1, \dots, n$. $V(X_i, Z, d, r, \rho_1, \rho_2, \varphi^0)$ $i = 1, \dots, n$ are the theoretical values of potential anomaly at the points $X_i = 1, \dots, n$.

Geological Setting

The massive sulphide ore body at Rouez occurs in the clastic formations of the upper Prioerian; it outcrops among the Coevron synclines in the north and the Laval syncline in the south. These synclines are of Paleozoic age. This zone is related to the southern-eastern margin of the Mancelian that is characterized by granodiorite intrusives of Cadomian age. Fig. 7 shows the study area and its geology.

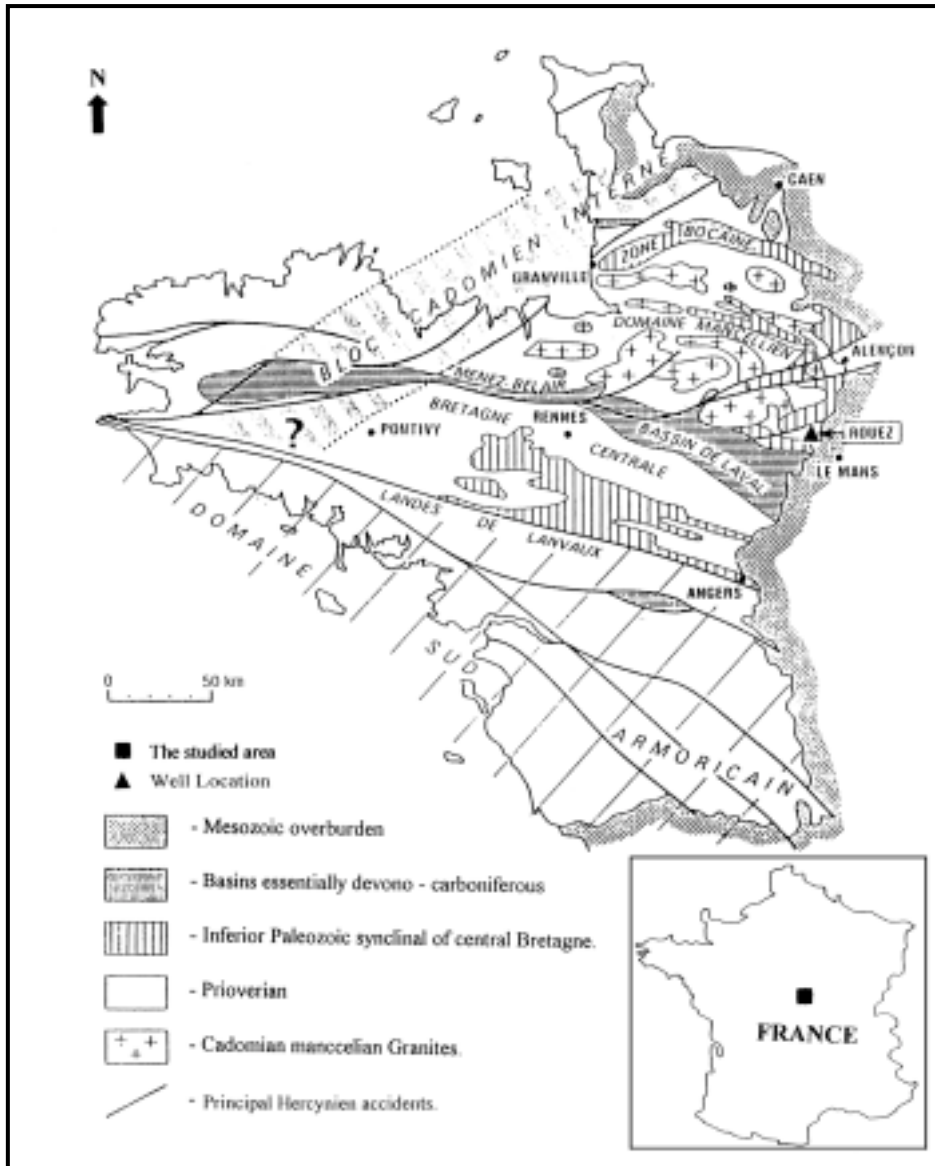


FIG. 7. The studied area and its geologic map.

On a local and regional scale the Prioerian formations consist of alternations of greywacke-silt-argillaceous silts and interbeddings of scattered lenses of intraformational conglomerates. Prioerian formations have undergone moderate deformation accompanied by low-grade metamorphism, which may be attributed to the varsique orogeny.

Geological data acquired from the mineralized zone and adjacent formations was achieved through boreholes that permitted geometric and stratigraphic study to depths of 30 to 40 m. These mineralizations are of the stratiform type and are encountered in the lithological succession of argillaceous-silt, greywacke and schist, along with hydrothermal facies of laminated sericite argillite and sandstone-argillite containing pyrite. Major components of the ore body are pyrite-pyrrhotite seditite-sphalerite-chalcopyrite and galena. Schistosity-stratigraphy interrelation study applied to core samples and correlation among the boreholes contributed to the determination of the morphology of the ore body and adjacent formations. This ore body consists of 100-300 m long lenses with an estimated thickness of ten meters conformable with the bedding.

Measurements Executed

The objective of this research work is to develop geophysical prospecting methodologies for the detecting of deep conductors around and not intersected with the well, in particular hole to surface and telluric-telluric methods Asfahani, 1989 and 2001. Therefore, several kinds of geoelectrical measurements were made in well 32. Fig. 8 shows the locality of this well on the gravity map that indicates clearly the presence of a positive gravity anomaly of 2.6 milligals. The average density of the host rock is 2.7 g/cm^3 , while the density of the sulphide mass is 4.9 g/cm^3 (i.e., the contrast is in the order of 2.3 g/cm^3). The residual anomaly derived from Bouger anomaly by a simple eliminating of plan indicates a mineralized body with inclination towards the north. The location of well 32 related to the mineralized body is shown in Fig. 9, Fromaigeat, 1985. The studied depth in this well is vertical until 400 m; therefore, there is no need to take into account the inclination effect for the executed measurements. Beyond 400 m, the well starts to deviate; and the measurements were stopped at this depth.

The geophysical measurements conducted in well 32 included:

Resistivity, Using Different Configurations

The conventional resistivity geoelectrical well logging short (RSN) and long normal (RLN) allow to divide generally the lithological studied section of well 32 into the following three zones, Asfahani, 1989, Fig 10:

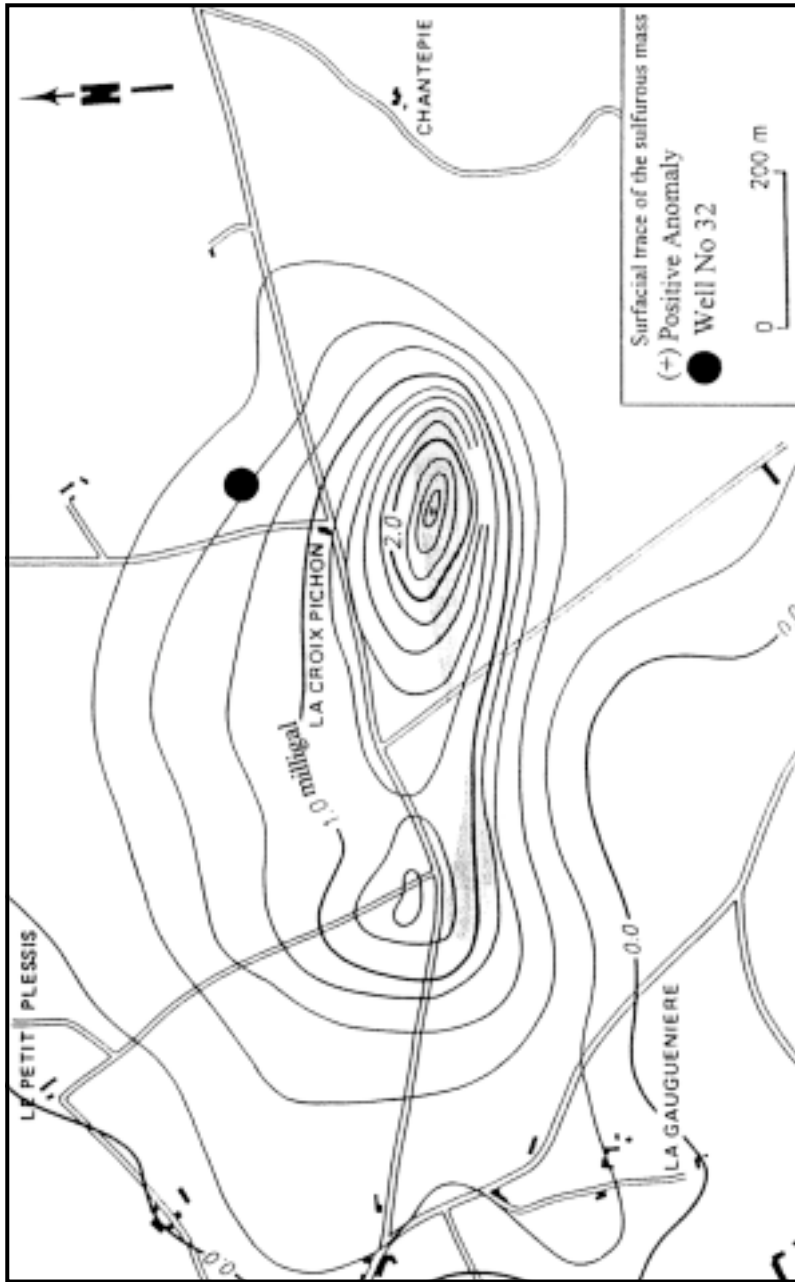


FIG. 8. The locality of the well 32 on the gravimetric map.

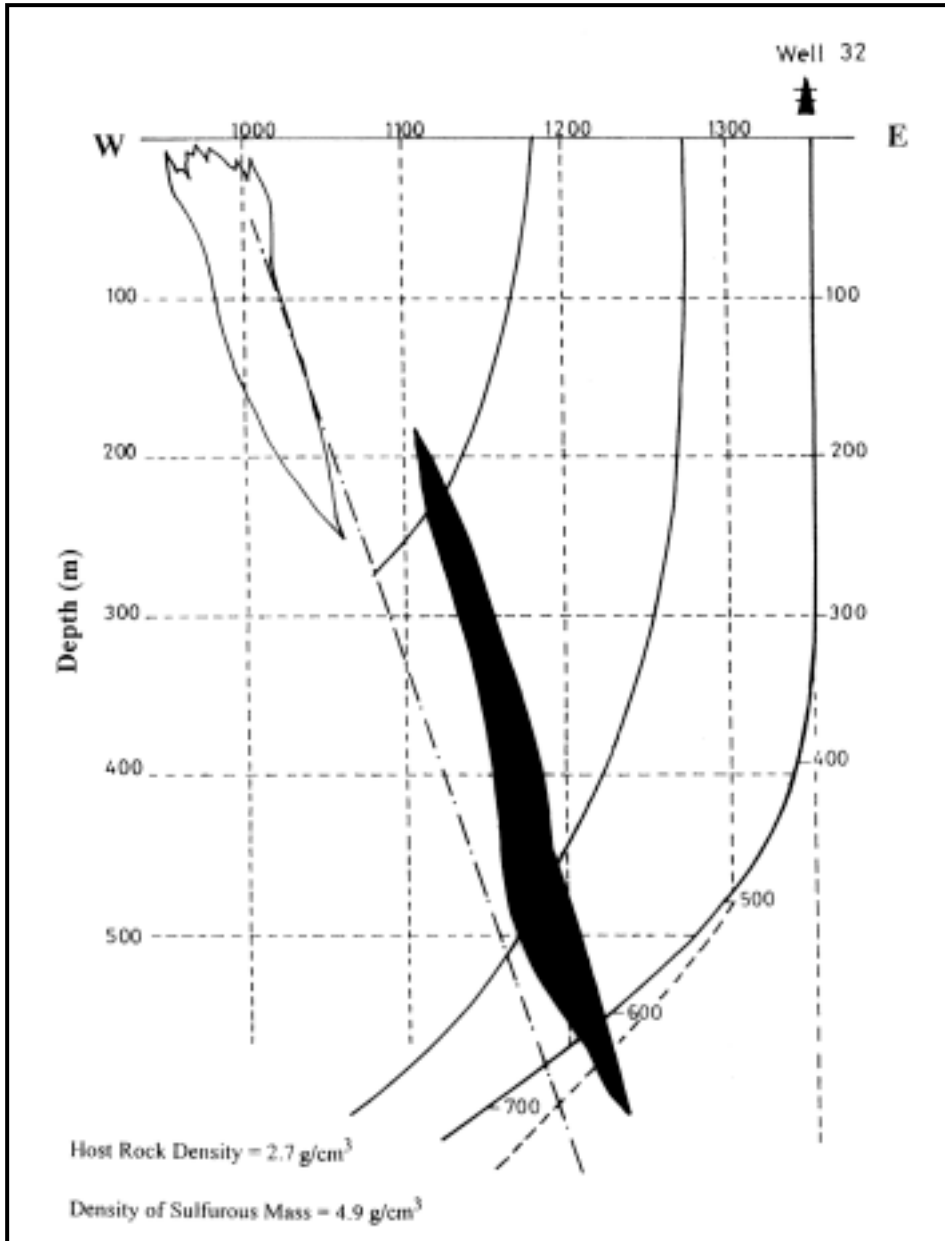


FIG 9. The position of the well 32 related to the mineral body.

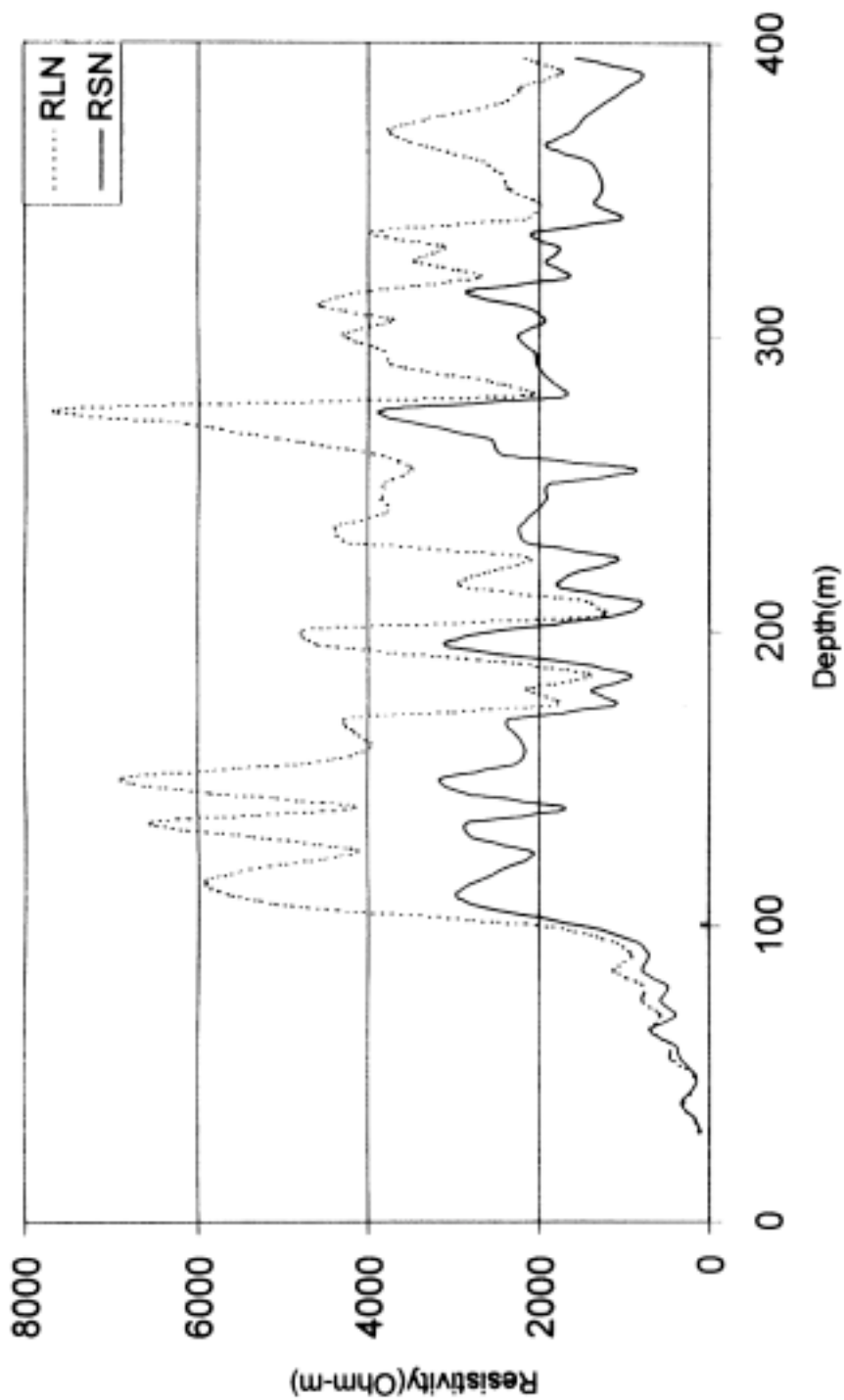


FIG 10. Resistivity measurements obtained in the well 32, using short and long normal.

1 – The first zone (from the surface to the depth of 100 m) is considered as a conductor zone, and is characterized by the presence of Eocene cover, pelite and the alteration product of pelites and siltite.

2 – The second zone (100-280 m) is a resistant zone with the presence of conductive paths, which are located at the depths of 110, 130, 165, 180, 200, 220 and 280 m, and are due to the presence of chlorite and disseminated pyrite traces.

3 – The third zone (280-400 m) is considered as a hydrothermal relatively conductive zone. The conductive paths are located at the depths of 310, 340 and 390 m, and are due to the presence of hematite, chlorite and pyrite.

Induced Polarization Measurements

These measurements have been carried out in time and frequency domains applying special geoelectrical configuration with a geometric coefficient of 2.67 m. This configuration consists of injecting the electrical current between two electrodes A and B spaced 10 m, and measuring the potential difference between other two electrodes *M* and *N* spaced 3 m, all the four mentioned electrodes are logged in the well.

Telluric-telluric Measurements

The measurements which are obtained by using the telluric-telluric method that are recently developed in the domain of wells are extensively explained in Asfahani, 2001.

Directional Measurements Using Hole to Surface Configuration

This new configuration is originally developed for detecting the deep conductors not intersected with the well. The superiority of such a configuration is due to its high penetration depth and to the obtained directional effect. In this research, the distance "*L*" between the two electrodes of injected current A and B in the surface was chosen to be 360 m, while the distance between the two electrodes *M* and *N* in the well was chosen to be 10 m.

Fig. 11 indicates the secondary vertical gradient curves obtained in the well 32, corresponding to the two perpendicular directions of injection current, EW and NS.

These data were corrected for the attenuation phenomena, Fig. 12, and subjected to the three types of filters described previously, where three types of anomalies have been distinguished in well 32. These anomalies are:

1 – Anomalies resulted from mineralized bodies that existed near but not intersected by well 32. These anomalies are characterized by short wavelengths,

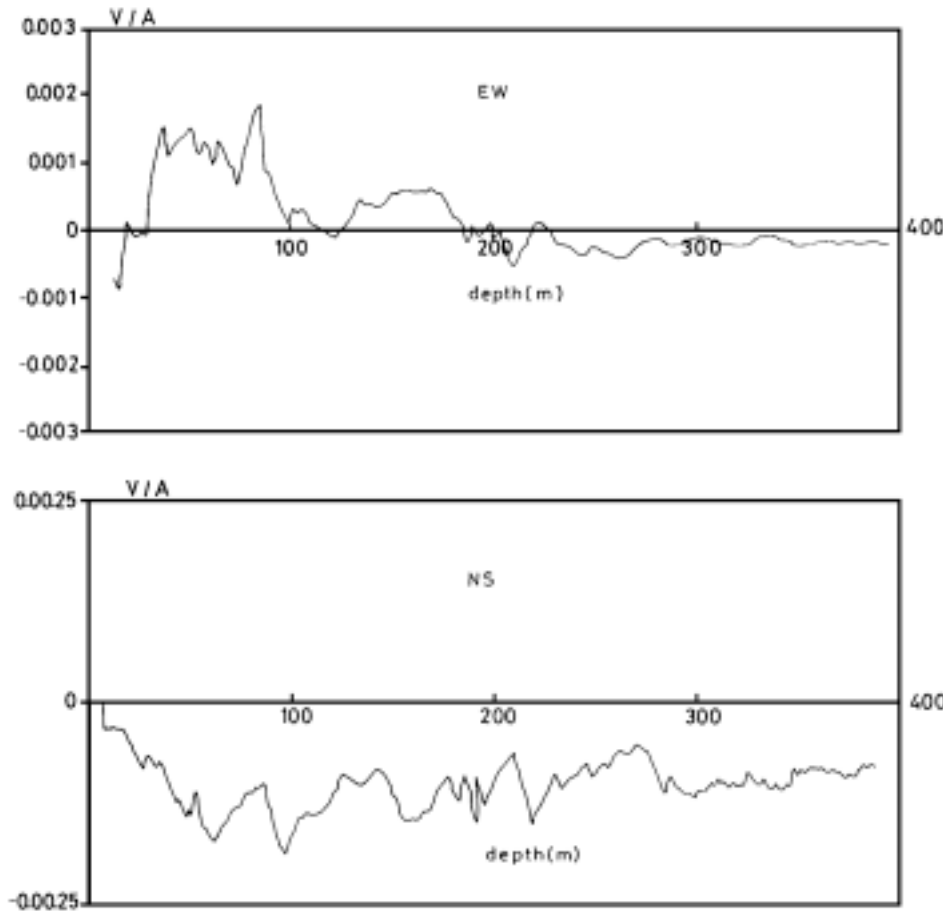


FIG. 11. Secondary vertical gradient curves obtained in the well 32, according to the EW, and NS current injections respectively.

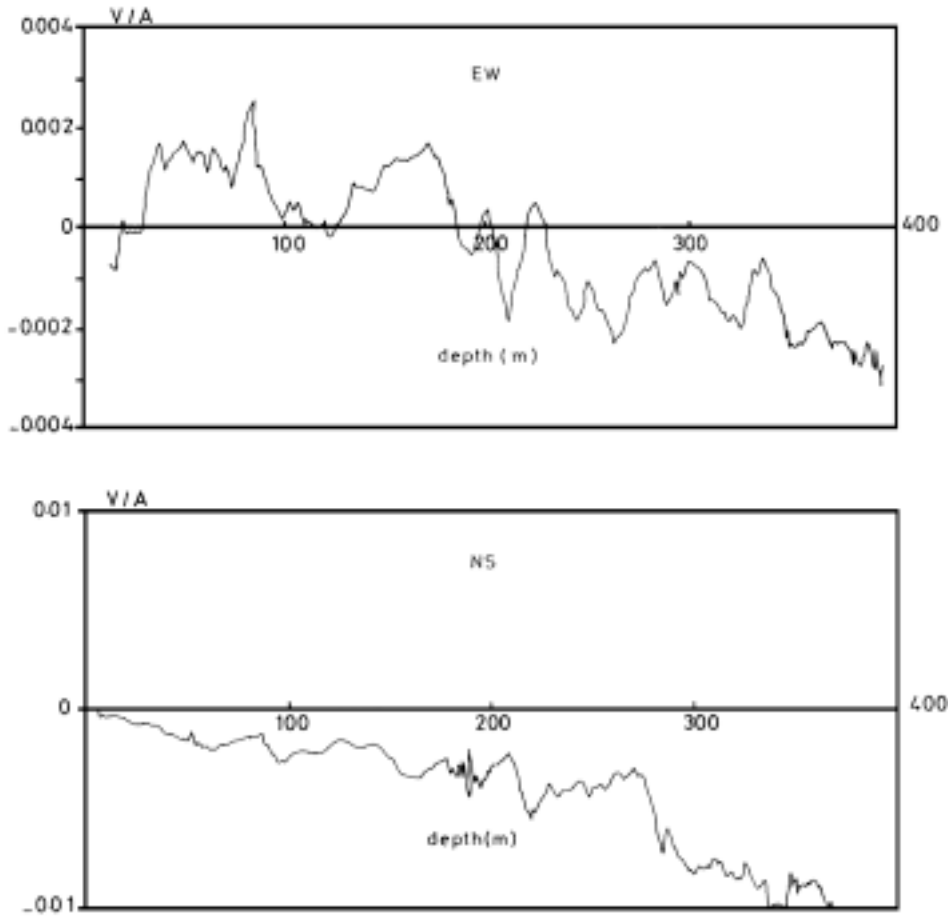


FIG. 12. Secondary vertical gradient curves obtained in the well 32, corrected for the attenuation phenomenon, according to the EW, and NS current injections respectively.

and identified as C1, C2 and C3 at the depths of 180 m, 210 m and 280 m respectively, Fig. 13. The selection of these anomalies was carried out by the application of a filter of $4 < d < 16$ m. The presence of these anomalies were confirmed by the traditional geoelectrical well logging, short and long normal, Fig. 10.

2 – Anomalies that resulted from mineralized bodies are identified as B1 and B2. These two anomalies existed at the depths of 190 m and 285 m respectively are characterized by mean wavelengths and selected by using a filter of $16 < d < 64$ m, Fig. 14. These anomalies will be treated using Chart method developed by Florsh, 1986.

3 – Anomalies resulted from mineralized bodies located at a large distance from the well 32, comparing with the two first kinds of anomalies, and identified as A1 and A2, Fig. 15. These anomalies are characterized by long wavelengths, and selected by using a low pass filter of $d > 64$ m.

They have an origin, which is difficult to be determined precisely, or their presence could be related to the tectonic effects. Using an inverse method developed in this research work will treat these two anomalies.

Summary of Geophysical Results Obtained in Well 32

The application of the diverse geoelectrical methods mentioned above, and their interpretation in well 32 allow summarizing the obtained results as follows:

*The ten conductive paths at the depths of (110, 130, 165, 180, 200, 220, 280, 310, 340 and 390 m) detected by conventional resistivity, short and long normal, (Fig. 10), are conductors intersected with well 32. The conductor detected at the depth of 210 m indicates a clear induced polarization anomaly, which could be related to the sulfide mineralization presence.

**All the conductors detected by both the telluric-telluric method, and the conventional resistivity logging method indicate probably that these conductors have lateral extension more important than the conductors detected only by conventional resistivity logging.

***Three types of conductors have been distinguished by applying filtering technique.

Fig. 16 shows all the conductors detected around well 32, by the application of diverse geophysical methods described in this paper.

Two separated mineralized zones were distinguished at the depths of 210 m and 280 m, which correspond probably to the conductors having big lateral extensions towards the West and Northeast respectively.

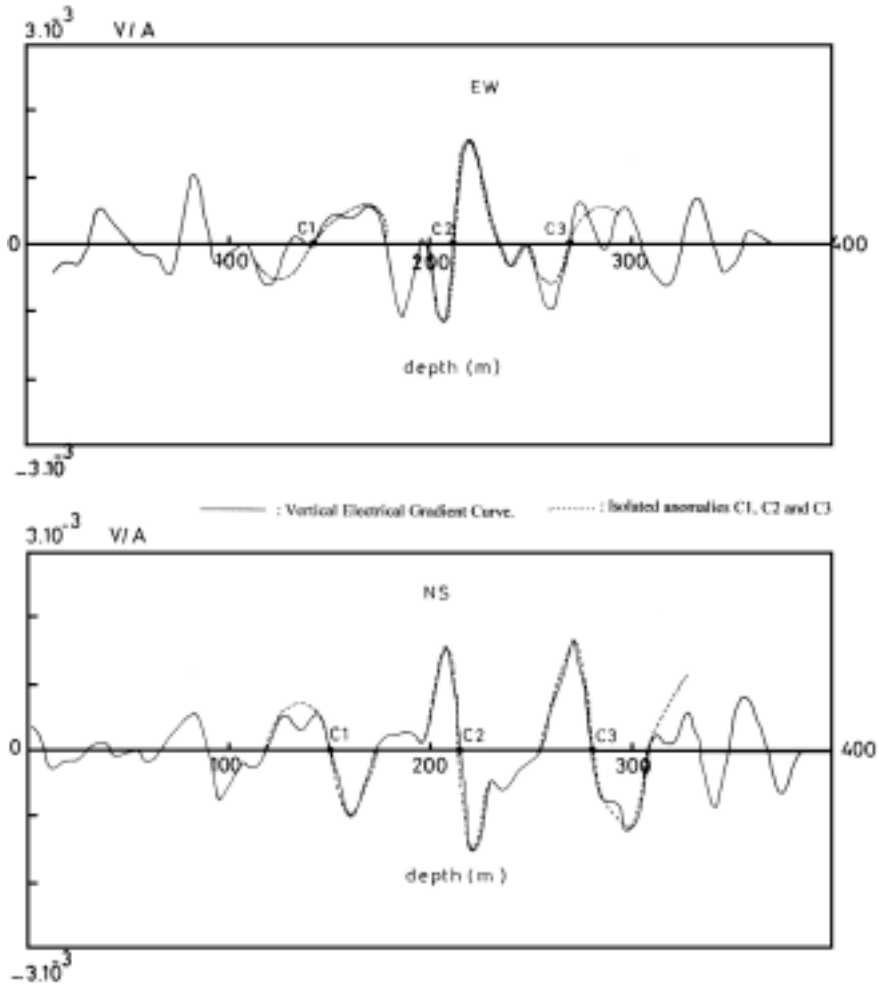


FIG 13. Corrected vertical gradient curves obtained in the well 32, filtered by the filter of $4 < d < 16$ m, according to the EW, and NS current injections respectively.

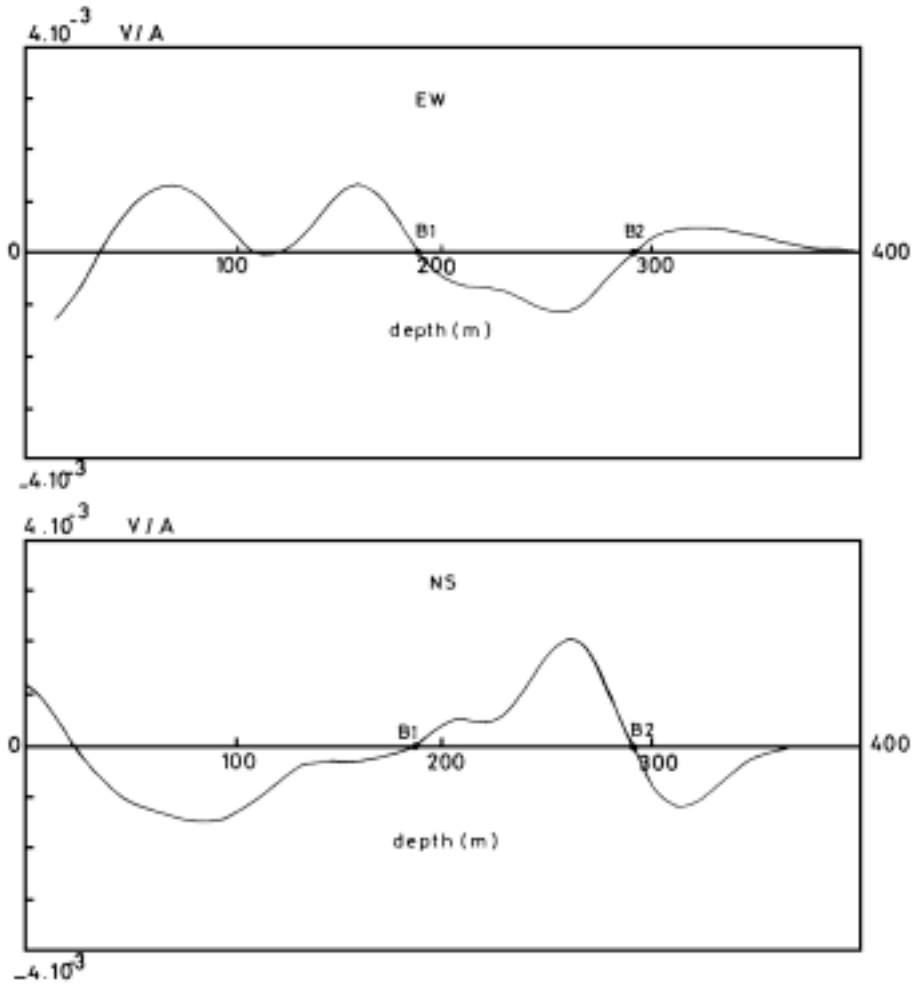


FIG. 14. Corrected vertical gradient curves obtained in the well 32, filtered by the filter of $16 < d < 64$ m, according to the EW, and NS current injections respectively.

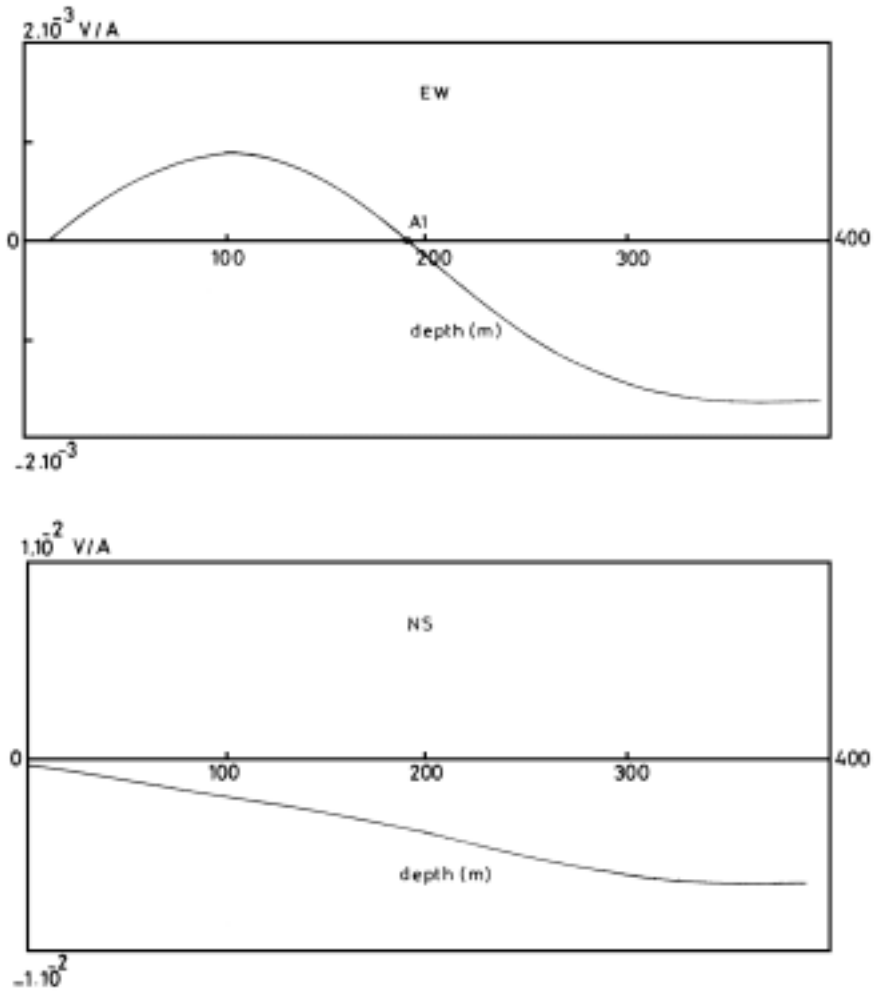


FIG. 15. Corrected vertical gradient curves obtained in the well 32, filtered by the filter of $d > 64$ m, according to the EW, and NS current injections respectively.

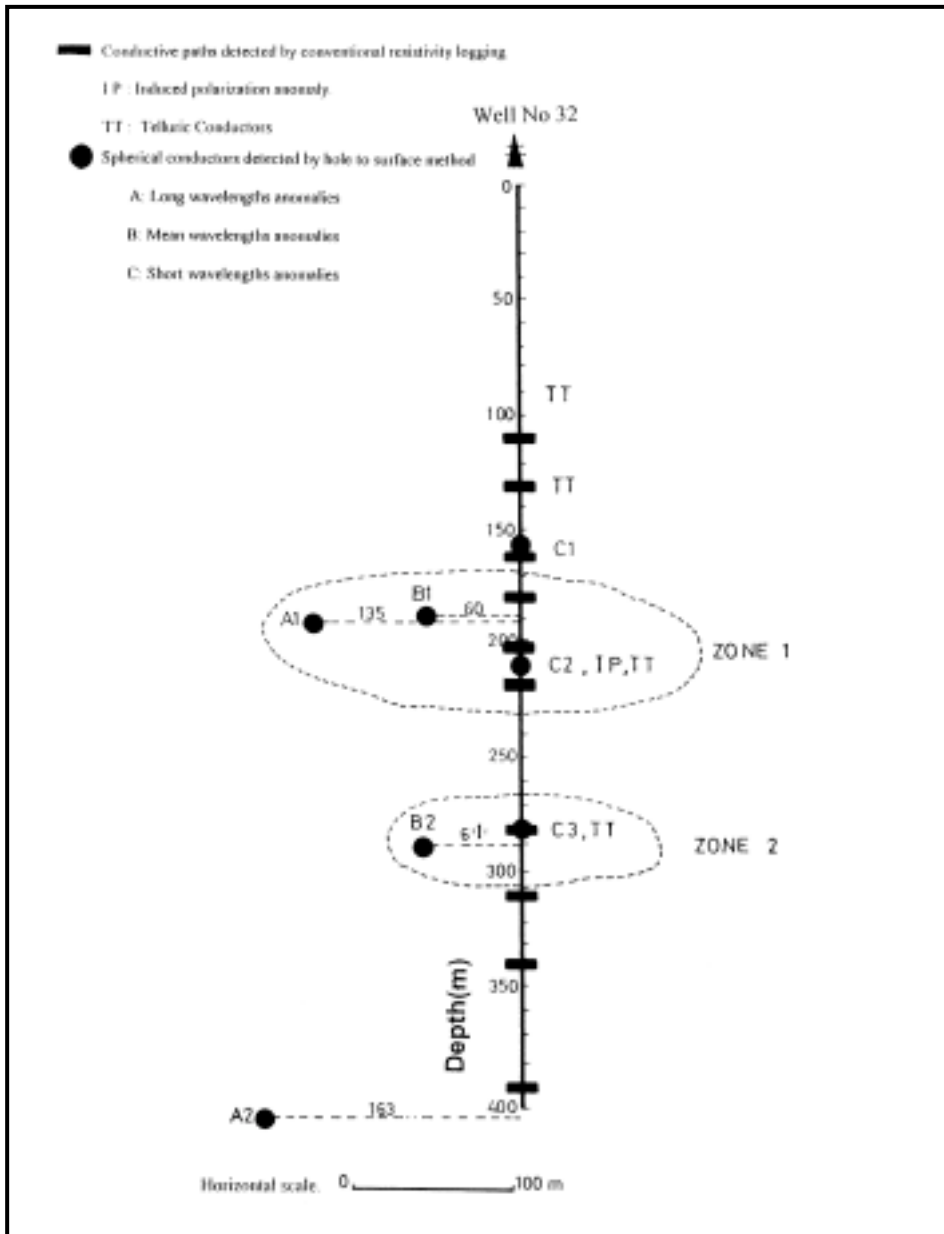


FIG. 16. The detected conductors around the well 32 obtained by the new configuration and other geoelectrical methods (Telluric-Telluric, Induced Polarization, and Resistivity logging).

Results And Discussions

Being a new configuration, the obtained field data have been interpreted using several interpretative techniques. Three types of anomalies have been distinguished by applying filtering technique. The first type of anomalies is characterized by short wavelengths. The presence of these anomalies identified as C1, C2, and C3 is confirmed by traditional geoelectrical well logging short and long normal, Figs. 13, and they have not been quantitatively interpreted.

The second type of anomalies identified as B1 and B2 has been quantitatively interpreted using chart method. The third type of anomalies identified as A1 and A2 has been interpreted using an inverse method.

B1 Anomaly

This anomaly has been well defined as it is shown in Fig. 14, and the qualitative examination indicates that this anomaly is situated in the third zone, Fig. 4-a. Its quantitative interpretation necessitates the following input data, which could be obtained directly from Fig. 14.

Cross over depth corresponding to this anomaly: $C = 190 \text{ m}$

The distance between the two extremes: $d = 60 \text{ m}$

$$\bar{A}_{EW} = 1.2 * 10^{-3}, \bar{A}_{NS} = 0.3 * 10^{-3}, \bar{A} = \sqrt{\bar{A}_{EW}^2 + \bar{A}_{NS}^2} \Rightarrow \bar{A} = 1.24 * 10^{-3}$$

$$\rho_1 = 2000 \Omega.m; \rho_2 = 0 \Omega.m; L = 360m; I = 0.994 \text{ Amp.}$$

$$\Rightarrow \frac{\bar{A} L^2}{I \rho_1} = 0.08; \frac{C}{L} = 0.53; \frac{d}{L} = 0.17$$

According to the charts A and B (Fig. 6), we have:

$$\frac{r}{L} = 0.08 \Rightarrow r = 29 \text{ m}, \frac{C}{L} = 1.04 \Rightarrow Z = 183 \text{ m}$$

$$\varphi = \arctg \frac{0.3}{1.2} = 14^\circ$$

B2 Anomaly

This anomaly has been well defined as it is shown in Fig. 14, and the qualitative examination indicates that this anomaly is situated in the first zone, Fig. 4-a. The input data needed for the quantitative interpretation could be obtained from Fig. 14:

Cross over depth corresponding to this anomaly: $C = 285$ m

$$A_{EW} = 1.1 * 10^{-3}; A_{NS} = 2 * 10^{-3}; A = 2.3 * 10^{-3}$$

The distance between the two extremes: $d = 61$ m

$$\rho_1 = 2000 \Omega \cdot m; \rho_2 = 0 \Omega \cdot m; L = 360 m; I = 0.994 \text{ Amp.}$$

$$\Rightarrow \frac{\bar{A} L^2}{I \rho_1} 0.15; \frac{C}{L} = 0.8; \frac{d}{L} = 0.17$$

According to the charts A and B, Fig. 6, we have:

$$\frac{r}{L} = 0.15 \Rightarrow r = 54 m; \frac{C}{Z} = 1 \Rightarrow Z = 285 m$$

$$\varphi = \arctg \frac{2}{1.1} 61^\circ$$

The interpretation results of the two anomalies B1 and B2 are summarized in Table 1.

TABLE 1. The results of chart method.

Anomaly	Depth $Z(m)$	Azimuth φ^0	Distance $d(m)$	Radius $r(m)$	ρ_1 ($\Omega \cdot m$)	ρ_2 ($\Omega \cdot m$)	Remarks
B1	183	14	60	29	2000	0	B1 exists more precisely towards the West.
B2	285	61	61	54	2000	0	B2 exists more precisely towards the North.

Using an inverse method developed in this research work with an adapted spherical model, we are able to determine the target depth (Z), distance to the well (d), radius (r) and the resistivity of the sphere (ρ_2), in addition to the resistivity of the host rocks (ρ_1). This method is applied her to interpret only the large anomalies resulted from mineral bodies, existed at large distance from the well 32 (A1 and A2), Fig. 15. Qualitative study of these two anomalies indicates the presence of an anomaly in the EW gradient curve at the depth of 190 m. In the NS gradient curve, it is not observed the presence of the same anomaly at the depth of 190 m. However, the form of the NS gradient curve indicates that this curve is incomplete, and it is possible, that it reaches a minimum at a depth more than 400 m (our measurements are stopped at 400 m). This minimum if it exists possibly indicates the presence of a mineral body (A2). Therefore, each of these two anomalies has been separately interpreted by an inverse method, and not been interpreted by chart method, which necessitates two gradient curves, representing the same anomaly.

We did not directly use the corrected vertical curves in this interpretation; instead these curves themselves are first transformed into potential curves by an integration procedure, using Simpson's Rule. In fact, the study of the obtained potential curves is preferable in this case, because the rapid variations which appear on vertical gradient curves are eliminated in potential curves, Fig. 17. Fig. 18 indicates the results of the inversion method for the two potential curves, EW and NS, which can also be summarized in Table 2.

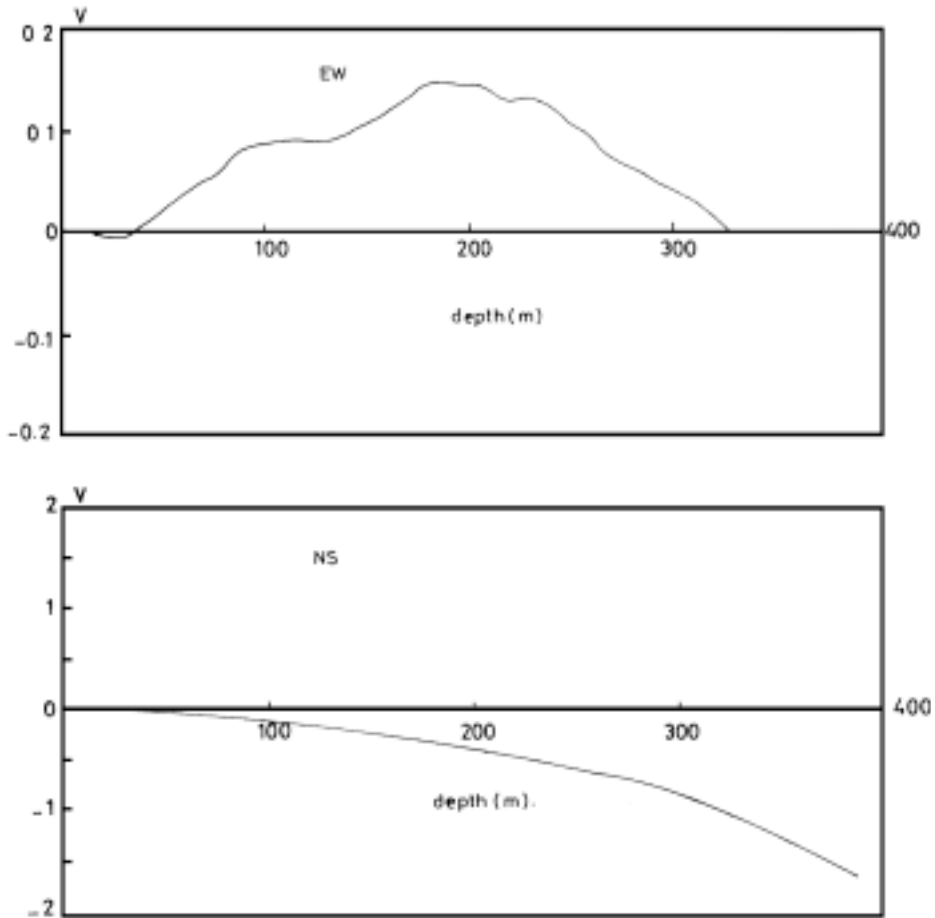


FIG. 17. The potential curves obtained in the well 32, according to the EW, and NS current injections respectively.

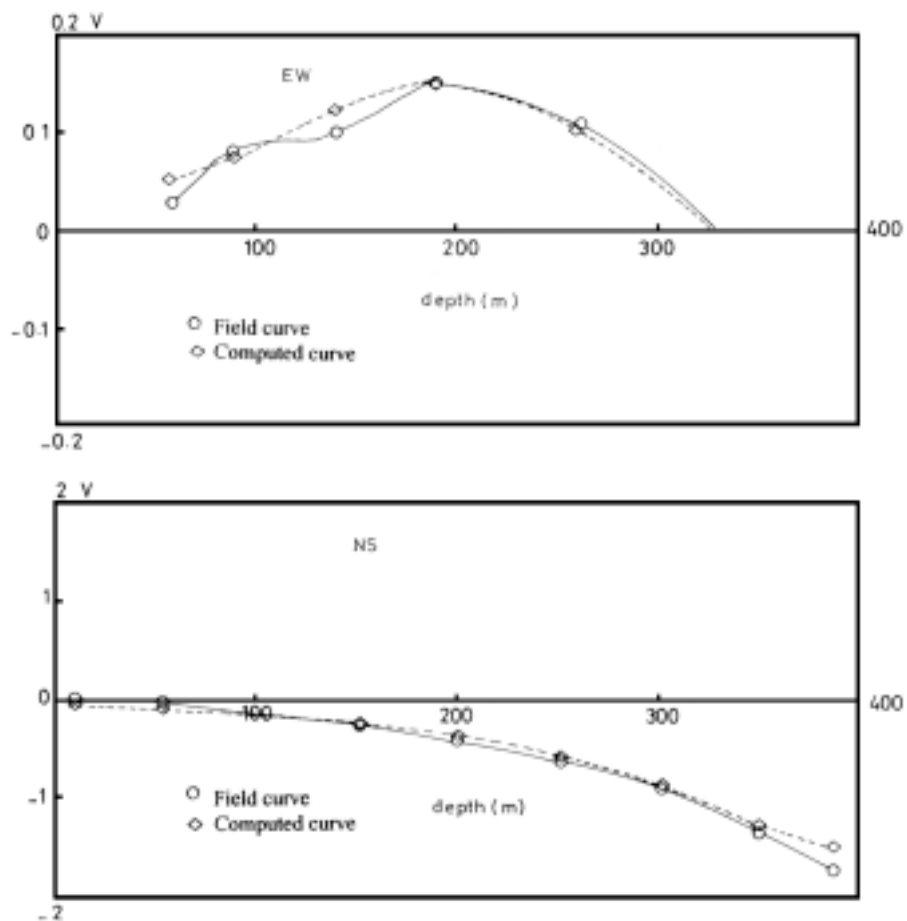


FIG. 18. Results of the inversion method applied to the potential curves, according to the EW, and NS current injections respectively.

TABLE 2. The results of the inversion method.

Interpreted curve	Distance $d(m)$	Depth $Z(m)$	Radius $r(m)$	ρ_1 ($\Omega \cdot m$)	ρ_2 ($\Omega \cdot m$)	Azimuth ϕ^0	Remarks
EW potential curve (A1)	135	190	31	2000	10	Exists in the EW plane	A1 exists more precisely towards the W
NS potential curve (A2)	163	413	74	2000	10	Exists in the NS plane	A2 exists more towards the S.

It is interesting to note that the EW potential curves interpreted by inversion method are the same anomalies obtained by the filter of $d > 64$ m, Fig. 15. In fact, this filter eliminated all the short wavelength anomalies. The response consists of only one anomaly, having its cross-over at the depth of 190 m, when the current is injected in EW direction. This interpretation must to be considered only as an equivalent theoretical model. Taking into account that the geological structure responsible of these potential anomalies in the two cases discussed above may be very different from the spherical structure supposed in the inversion process. They are probably due to a tectonic or lithological cause.

Finally, Fig. 19 indicates the detected conductors resulted from several interpretative techniques applied to the data obtained by applying the new hole to surface configuration in Rouez mine.

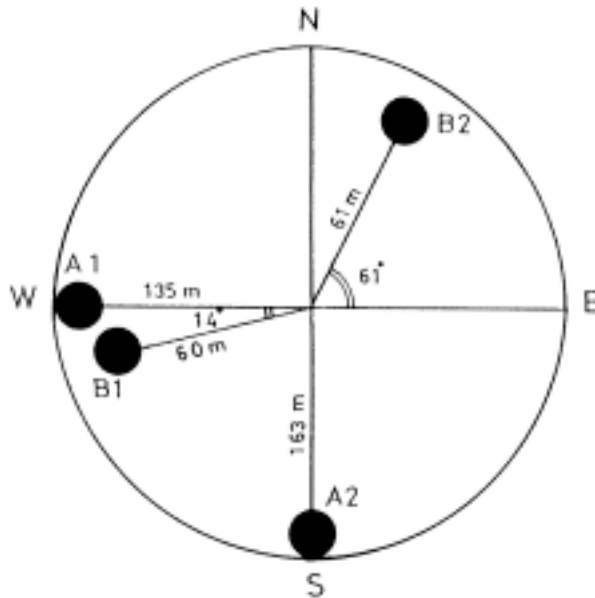


FIG. 19. Detected conductors around the well 32, obtained by the new well to surface configuration.

Conclusion

A new geoelectrical hole to surface configuration is proposed in this research for the detecting of deep conductors, not-intersected with the well. The advantage and the superiority of such a configuration are related to the fact that it is characterized by high penetration depth and offers a directional effect.

The economic importance of this configuration is demonstrated, since it decreases the number of wells, which are necessary for the detecting of spreaded conductors. The application of this configuration gives an idea about the loca-

tion of the conductors in the plane, which allows proposition of a suitable strategy to extend the prospecting zone in the area under study. This configuration is successfully tested and practiced in Rouez mine in France. More practical measurements have to be carried out using this configuration, in order to approve its effective detection and to make it an active configuration, easily used in mining and prospecting fields.

Acknowledgments

Professor Pham Van Ngoc from Institute de Physique de Globe de Paris (IPGP)-France is gratefully thanked, for providing the facilities and equipments for conducting the geoelectrical measurements presented in this paper.

Dr. Danielle Boyer from IPGP is also thanked for her collaboration in the field. Special thanks to the editors and the reviewers for their keen interest, valuable comments on the manuscript and constructive suggestions for the improvements the quality of this paper.

References

- Asfahani, J.** (1989) Methodologies de prospection uranifere a grande profondeur par les mesures geoelectriques en surface et dans les trous de forage. *Thèse doctorat- I.N.P.L.*, Nancy-France.
- Asfahani, J.** (2001) New method in telluric prospecting for detecting deep conductors, not intersecting with wells. Application in the Rouez region (France). *JKAU: Earth Science* (in Press).
- Daniels, J.J.** (1978): Interpretation of buried electrode resistivity data using a layered earth model. *Geophysics*, **43**: 988-1001.
- Daniels, J.J.** (1983) Hole to surface measurements. *Geophysics*, **48**: 87-97.
- Dobecki, T.I.** (1980) Borehole resistivity curves near spheroidal masses, *Geophysics*, **45**: 1513-1522.
- Florsh, N.** (1986) Nouvelle methodologie electrique pour la detection a distance autour des trous de forages. *Thèse doctorat-I.N.P.L.*, Nancy-France.
- Fromaigeat, L.** (1985) Méthode electromagnetique en forage: application de la mesure des trois composantes magnetiques en exploration minière. *Thèse doctorat-I.N.P.L.*, Nancy-France.
- Gradshteyn, I.S. and Ryzhik, I.M.** (1969) *Table of integrals, series and products*, Academic Press.
- Yang, F.W. and Ward, S.H.** (1985) On sensitivity of surface to borehole resistivity measurements to the attitude and depth to center of a three dimensional spheroid, *Geophysics*, **50**: 1173-1178.

تشكيل جيوكهربائي جديد من السطح إلى البئر لكشف النواقل العميقة حول الآبار المحفورة باستخدام التيار المتواصل حالة دراسة من منجم رويز-بريتان-فرنسا

جمال عبده أصفهاني

قسم الجيولوجيا ، هيئة الطاقة الذرية

دمشق - سوريا

المستخلص . تم اقتراح تشكيل جيوكهربائي جديد يتم بموجبه قياس مركبة الحقل الكهربائي العمودي داخل البئر الناتج عن حقن للتيار الكهربائي المتواصل على السطح بشكل متناظر بالنسبة لموقع البئر. يتمتع هذا التشكيل بعمق اختراق كبير مقارنة مع أعماق الاختراق التي يتم الحصول عليها بالطرق الجيوكهربائية التقليدية المطبقة من على السطح وفي داخل الآبار. كما ويبيدي هذا التشكيل خاصة اتجاهاتية ، وهي واحد من أهم محسناته الهامة التي تبرهن على تفوقه. جرى اختبار هذا التشكيل في منجم رويز - بريتان - فرنسا ، حيث تتواجد تمعدنات للكبريت . تم من خلال القياسات الحقلية عزل العديد من الشاذات والتي فسرت باستخدام تقانات تفسيرية مختلفة. كانت النتائج التي تم الحصول عليها باستخدام هذا التشكيل متوافقة، إضافة إلى أن النواقل التي كشفت بهذه الطريقة يدعم وجودها الوصف الليثولوجي والمورفولوجي .